



Optimizing single mode robustness of the distributed modal filtering rod fiber amplifier.

Jørgensen, Mette Marie; Petersen, Sidsel Rübner; Laurila, Marko; Lægsgaard, Jesper; Alkeskjold, Thomas Tanggaard

Published in:
Optics Express

Link to article, DOI:
[10.1364/OE.20.007263](https://doi.org/10.1364/OE.20.007263)

Publication date:
2012

Document Version
Publisher's PDF, also known as Version of record

[Link back to DTU Orbit](#)

Citation (APA):
Jørgensen, M. M., Petersen, S. R., Laurila, M., Lægsgaard, J., & Alkeskjold, T. T. (2012). Optimizing single mode robustness of the distributed modal filtering rod fiber amplifier. *Optics Express*, 20(7), 7263-7273.
<https://doi.org/10.1364/OE.20.007263>

General rights

Copyright and moral rights for the publications made accessible in the public portal are retained by the authors and/or other copyright owners and it is a condition of accessing publications that users recognise and abide by the legal requirements associated with these rights.

- Users may download and print one copy of any publication from the public portal for the purpose of private study or research.
- You may not further distribute the material or use it for any profit-making activity or commercial gain
- You may freely distribute the URL identifying the publication in the public portal

If you believe that this document breaches copyright please contact us providing details, and we will remove access to the work immediately and investigate your claim.

Optimizing single mode robustness of the distributed modal filtering rod fiber amplifier

Mette Marie Jørgensen,^{1,*} Sidsel Rübner Petersen,¹ Marko Laurila,¹ Jesper Lægsgaard,¹
and Thomas Tanggaard Alkeskjold²

¹DTU Fotonik, Department of Photonics Engineering, Technical University of Denmark, 2800 Kgs. Lyngby, Denmark

²NKT Photonics, Blokken 84, 3450 Birkerød, Denmark

*mmajo@fotonik.dtu.dk

Abstract: High-power fiber amplifiers for pulsed applications require large mode area (LMA) fibers having high pump absorption and near diffraction limited output. Photonic crystal fibers allow realization of short LMA fiber amplifiers having high pump absorption through a pump cladding that is decoupled from the outer fiber diameter. However, achieving ultra low NA for single mode (SM) guidance is challenging, thus different design strategies must be applied. The distributed modal filtering (DMF) design enables SM guidance in ultra low NA fibers with very large cores, where large preform tolerances can be compensated during the fiber draw. Design optimization of the SM bandwidth of the DMF rod fiber is presented. Analysis of band gap properties results in a fourfold increase of the SM bandwidth compared to previous results, achieved by utilizing the first band of cladding modes, which can cover a large fraction of the Yb emission band including wavelengths of 1030 nm and 1064 nm. Design parameters tolerating refractive index fabrication uncertainties of $\pm 10^{-4}$ are targeted to yield stable SM bandwidths.

©2012 Optical Society of America

OCIS codes: (060.4005) Microstructured fibers; (060.2280) Fiber design and fabrication; (060.2320) Fiber optics amplifiers and oscillators.

References and links

1. D. J. Richardson, J. Nilsson, and W. A. Clarkson, "High power fiber lasers: current status and future perspectives [Invited]," *J. Opt. Soc. Am. B* **27**(11), B63–B92 (2010).
2. J. Limpert, F. Röser, S. Klingebiel, T. Schreiber, C. Wirth, T. Peschel, R. Eberhardt, and A. Tünnermann, "The rising power of fiber lasers and amplifiers," *IEEE J. Sel. Top. Quantum Electron.* **13**(3), 537–545 (2007).
3. W. Wadsworth, R. Percival, G. Bouwmans, J. Knight, and P. Russell, "High power air-clad photonic crystal fibre laser," *Opt. Express* **11**(1), 48–53 (2003).
4. J. Limpert, A. Liem, M. Reich, T. Schreiber, S. Nolte, H. Zellmer, A. Tünnermann, J. Broeng, A. Petersson, and C. Jakobsen, "Low-nonlinearity single-transverse-mode ytterbium-doped photonic crystal fiber amplifier," *Opt. Express* **12**(7), 1313–1319 (2004).
5. C.-H. Liu, G. Chang, N. Litchinitser, D. Guertin, N. Jacobsen, K. Tankala, and A. Galvanauskas, "Chirally coupled core fibers at 1550-nm and 1064-nm for effectively single-mode core size scaling," *OSA Technical Digest Series (CD)*, paper CTuBB3 (2007).
6. S. Lefrançois, T. S. Sosnowski, C.-H. Liu, A. Galvanauskas, and F. W. Wise, "Energy scaling of mode-locked fiber lasers with chirally-coupled core fiber," *Opt. Express* **19**(4), 3464–3470 (2011).
7. F. Jansen, F. Stutzki, H.-J. Otto, M. Baumgartl, C. Jauregui, J. Limpert, and A. Tünnermann, "The influence of index-depressions in core-pumped Yb-doped large pitch fibers," *Opt. Express* **18**(26), 26834–26842 (2010).
8. F. Jansen, F. Stutzki, H.-J. Otto, T. Eidam, A. Liem, C. Jauregui, J. Limpert, and A. Tünnermann, "Thermally induced waveguide changes in active fibers," *Opt. Express* **20**(4), 3997–4008 (2012).
9. F. Jansen, F. Stutzki, C. Jauregui, J. Limpert, and A. Tünnermann, "Avoided crossings in photonic crystal fibers," *Opt. Express* **19**(14), 13578–13589 (2011).
10. J. Fini, "Design of solid and microstructure fibers for suppression of higher-order modes," *Opt. Express* **13**(9), 3477–3490 (2005).
11. T. Murao, K. Saitoh, and M. Koshiba, "Multiple resonant coupling mechanism for suppression of higher-order modes in all-solid photonic bandgap fibers with heterostructured cladding," *Opt. Express* **19**(3), 1713–1727 (2011).
12. T. T. Alkeskjold, M. Laurila, L. Scolari, and J. Broeng, "Single-Mode ytterbium-doped Large-Mode-Area photonic bandgap rod fiber amplifier," *Opt. Express* **19**(8), 7398–7409 (2011).

13. M. Laurila, J. Saby, T. T. Alkeskjold, L. Scolari, B. Cocquelin, F. Salin, J. Broeng, and J. Lægsgaard, "Q-switching and efficient harmonic generation from a single-mode LMA photonic bandgap rod fiber laser," *Opt. Express* **19**(11), 10824–10833 (2011).
 14. J. Lægsgaard, "Gap formation and guided modes in photonic bandgap fibres with high-index rods," *J. Opt. A* **6**(8), 798–804 (2004).
 15. M. Laurila, M. M. Jørgensen, K. R. Hansen, T. T. Alkeskjold, J. Broeng, and J. Lægsgaard, "Distributed mode filtering rod fiber amplifier delivering 292W with improved mode stability," *Opt. Express* **20**(5), 5742–5753 (2012).
 16. S. Selleri, L. Vincetti, A. Cucinotta, and M. Zoboli, "Complex FEM modal solver of optical waveguides with PML boundary conditions," *Opt. Quantum Electron.* **33**(4/5), 359–371 (2001).
-

1. Introduction

Rare-earth-doped fiber optical amplifiers allow high brightness and excellent mode quality due to fiber beam confinement [1–4]. In addition, good thermal handling is achieved due to the large ratio of surface area to active volume. Nonlinearities set the main limitations for increasing peak power and pulse energy, motivating the possibility to increase the effective mode area. However, the fiber core area cannot be increased unlimited, since single mode (SM) performance is crucial for maintaining diffraction limited focus ability and high beam pointing stability. Degradation of beam quality is a critical factor for future power scaling of fiber optical lasers and amplifiers. An all solid fiber with chirally-coupled cores (CCC) has been demonstrated to increase the core diameter up to 33.5 μm and have effective SM operation by coupling all higher order modes (HOMs) of the central core into high-loss helix side modes [5, 6]. The CCC fiber is dependent on fabrication parameters of the helix side core and further core scaling has yet to be seen.

In photonic crystal fibers (PCFs) large core areas and double clad structures can be combined. The advantage of the PCF is utilized in the large pitch fiber (LPF) design, which essentially is a one cell core PCF design with a large pitch yielding core sizes in the range of 53 – 107 μm [7, 8]. The modes are weakly confined to the core in the LPF, which induces a sufficient differential loss between the fundamental mode (FM) and HOMs. However, the FM properties of the LPF design are extremely sensitive to fabrication variations in for instance the core refractive index [9], variations that are caused by doping of Yb. Compensation of core refractive index changes is important in the active large mode area (LMA) fiber to be used in a fiber amplifier configuration. Varying the effective cladding index during the fiber draw to yield a low numerical aperture (NA) can give the index compensation that result in SM operation. The double clad structure in a PCF gives the possibility for a pump cladding that is decoupled from the outer fiber diameter yielding controllable high pump absorption. Furthermore, high refractive index regions operating as resonators in PCFs can be placed in the inner cladding structure. The resonators can couple and create bands of cladding modes, which couple with core modes, whenever index matching is achieved [10, 11]. The distributed modal filtering (DMF) rod fiber utilizes resonators in the inner cladding structure to enable SM guidance over a certain spectral range despite the very LMA and ultra low NA [12]. High index resonators in a low index cladding function as modal filters filtering HOMs out of the core into the cladding [12, 13]. This enables very LMA fibers that maintain SM guidance over a certain spectral range, and has good beam quality and pointing stability in a fiber amplifier configuration. Efficient suppression of HOMs in straight very LMA fiber rods with ultra-low NA is challenging and require high precision on the effective refractive indices of the stacking elements. Air holes in the photonic crystal structure of the DMF rod fiber allow for high manufacturability, where fabrication uncertainties are compensated during the fiber draw.

In this paper, the DMF rod fiber is modeled numerically and a spectral window with SM behavior is identified and compared to the previous measurements in [12]. The distributed modal filtering effect is explained in Sec. 2 and the computational model is set up in Sec. 3. Simulations are performed on the original DMF rod fiber design and compared to previous measurements in Sec. 4. In Sec. 5 the DMF rod fiber is optimized by considering the band of cladding modes and utilizing the first band instead of the second to create an increase in relative SM bandwidth of approximately a factor of four, also taking fabrication uncertainties into consideration in Sec. 6. The pitch determines the core diameter, where a large increase

results in an unwanted increase in the core refractive index fabrication sensitivity, investigated in Sec. 7. The conclusions are given in Sec. 8.

2. Distributed modal filtering rod fiber

The DMF rod fiber is a hybrid fiber utilizing both total internal reflection (TIR) and the photonic band gap (PBG) effect. Air holes are placed in a triangular lattice in a silica background with up-doped Germanium rings (Ge-rings) surrounding some air holes placed in a kagome-type structure. 19 cladding cells are omitted creating the core. The air holes confine light by TIR and the up-doped Ge-rings form a band of cladding modes, which couple to core modes, whenever index matching is achieved, and thereby function as distributed modal filtering elements. The ring of air holes closest to the core ensures high mode quality of the FM by reducing coupling between the FM and the resonators, when the FM is well guided. An air cladding surrounds the inner cladding with a protective silica layer on the outside, enabling high pump absorption for the active DMF rod fiber in which the core is Yb-doped. The spectral placement of the index matching between core and resonator modes is determined by the size of the Ge-rings, which is controlled during the fiber draw by varying the air hole diameter. This allows spectral control of the SM bandwidth, contrary to a design with solid Ge-doped inclusions, where the size cannot be varied during the draw process [14].

Numerical computations allow for optimizing the DMF rod fiber to yield larger SM bandwidth and determine fabrication parameters to be used in the fiber draw. A definition of SM bandwidth is needed to compare design properties. This paper focuses on the FM and the first HOM to determine SM properties [7]. Previous experimental studies have shown SM properties of the DMF rod fiber within the spectral region, where the first HOM, resembling the first asymmetric LP_{11} -like HOM, couples with the resonators [12, 13]. This supports the argument that the first HOM is the limiting factor, also stated in [7]. Other HOMs might influence the SM bandwidth and further investigations must be conducted.

The effective refractive index of the first HOM must match the effective refractive index of the cladding modes to enable coupling. In this spectral region the first HOM is distributed over the entire inner cladding structure and not guided within the core. If the FM is confined to the core, the DMF rod fiber is SM. The SM bandwidth is the region, where the first HOM is leaking and couples with cladding modes, while the FM is still confined to the core and have a large fraction of modal power within the core. A general criterion for the SM bandwidth based on fraction of power in the core of the DMF rod fiber is chosen: a minimum FM core overlap of 80% is required together with a maximum 50% first HOM core overlap. These core overlap values provide good agreement between SM bandwidths of the simulated and fabricated DMF rod fiber as seen in Sec. 4. The criterion allows SM bandwidth comparisons and trend observations of different DMF rod fiber designs.

Recently, it has been shown that a temperature induced index change cause the SM bandwidth to slightly blueshift approximately 5 nm with a 157 W signal power [15]. This magnitude of the blueshifting is relatively small compared to the SM bandwidth, and this paper therefore focuses on the SM properties of the passive DMF rod fiber, and does not include any thermal effects. Including thermal effects is scope of further work.

3. Computational model

The quarter of the DMF rod fiber cross-section is modeled numerically with the finite element method, where each subdomain is specified by the refractive index [16]. The quadrilateral at the center is used as the core for the computations, although it has a slightly smaller area, than the internal region surrounded by the inner cladding structure, see Fig. 1. However for the active DMF rod fiber the area corresponds to the doped region of the core. The outer silica ring of the DMF rod fiber is not considered, since essentially the field is zero in this region. The air cladding of the DMF rod fiber is represented by a ring instead of a large number of air holes, and has a numerical aperture of 0.6 relative to silica, see Fig. 1. The field will decrease towards zero in the air cladding, meaning that the actual structure of the air cladding is unimportant. In the fabricated DMF rod fiber the air cladding confine all modes to the inner

cladding structure yielding low loss. Therefore it becomes important to consider core overlap for double clad PCFs instead of differential loss, since a simulated PML as the outer fiber boundary does not represent the physical fiber structure.

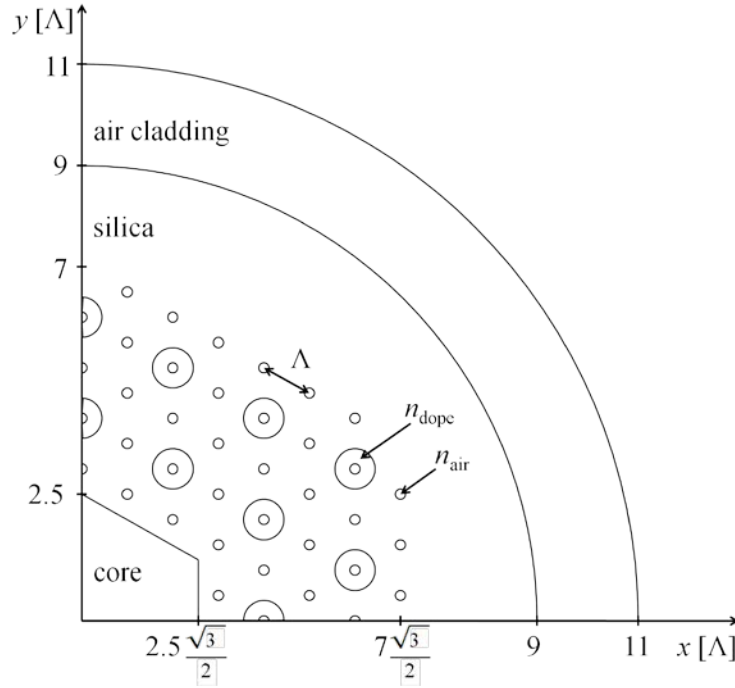


Fig. 1. The model of a quarter of the cross-section of the distributed mode filtered (DMF) rod fiber for numerical simulations. The core of the DMF rod fiber is defined by the quadrilateral at the center. The smallest circles represent air holes in the cladding structure with a refractive index of n_{air} , where some are surrounded by up-doped silica placed in a kagome-type lattice with refractive index n_{dope} . The outer ring represents the air cladding, and the pitch, Λ , is indicated as the center to center distance between two adjacent air holes.

A filling fraction, f , is introduced to ensure mass conservation of the DMF elements, yielding the ability to change the pitch and air hole diameter without increasing or decreasing the mass of the up-doped Ge-rings. The filling fraction, f , is given by the radius of the up-doped Ge-ring, r_{dope} , the air hole diameter, d , and the pitch, Λ :

$$f = \left(\frac{2r_{\text{dope}}}{\Lambda} \right)^2 - \left(\frac{d}{\Lambda} \right)^2. \quad (1)$$

If the pitch or air hole diameter changes in Eq. (1), r_{dope} must change as well to keep f constant. This allows the simulations to match variations in the fabricated DMF rod fiber, without adding or reducing the volume of the up-doped Ge-rings.

A scattering boundary condition is chosen for the outer fiber boundary, as the air cladding is forcing the field towards zero. Along the x - and y -axis either perfect electric conductor or perfect magnetic conductor is chosen, resulting in four different combinations, two for each axis that must be considered in order to determine all modes of the DMF rod fiber. The FM resembles the LP_{01} mode of a step index fiber and is the solution with the highest amount of power in the hexagonal core for two of the four combinations of boundary conditions, corresponding to the two polarizations of the FM. The first HOM is the solution with the highest amount of power in the hexagonal core for the other two set of boundary conditions. Thereby the FM and first HOM are distinguished by choosing different boundary conditions, and only two sets of boundary conditions are necessary to consider for determining SM

properties of the DMF rod fiber. To maximize FM gain and minimize HOM gain, the FM must have a large amount of power within the core in the SM bandwidth, where the first HOM must be suppressed within the core. Thus the fraction of modal core power is an important indicator for determining the spectral limits of the SM bandwidth. The z -component of the time average power flow of the core relative to the total cross-section yields the fraction of core power. Computations are conducted over a range of wavelengths.

4. Results for original design

The cross-section of the DMF rod fiber is modeled with a pitch of $14.5\ \mu\text{m}$ yielding a hexagonal core with a maximum width of $72.5\ \mu\text{m}$ and a maximum width within the inner cladding structure of approximately $84\ \mu\text{m}$. The air hole and resonator diameter relative to the pitch is 0.1 and 0.6 respectively, and the refractive index difference between the silica background and the up-doping of the Ge-rings is set to 2.5×10^{-3} .

Figure 2 shows the fraction of power in the core as a function of wavelength for the FM and two relevant LP_{11} -like modes. In the region where the FM couples with the resonators the fraction of core power drops off rapidly, likewise for the first HOM, LP_{11} . However the power level of an additional LP_{11} -like mode ($\text{LP}_{11}^{(2)}$) increases within the SM bandwidth that is the light blue region in Fig. 2. Comparing modal plot B and C in Fig. 2 it is noticed that the phase of the tails in the inner cladding of the two LP_{11} -like modes differ, clarifying that these are to different LP_{11} -like modes. A SM bandwidth is recognized from 946 nm to 963 nm, where the power level of the first HOM is below $\sim 50\%$, and the FM is well guided within the core, yielding a SM bandwidth of 1.8% relative to the center wavelength. The field distribution within the DMF elements in Fig. 2 resembles LP_{11} -like modes of a step index fiber if omitting the air hole at the center of one resonator. This implies that the second set of cladding modes is utilized to create the SM bandwidth, which is the second band gap created by the resonating Ge-rings [14].

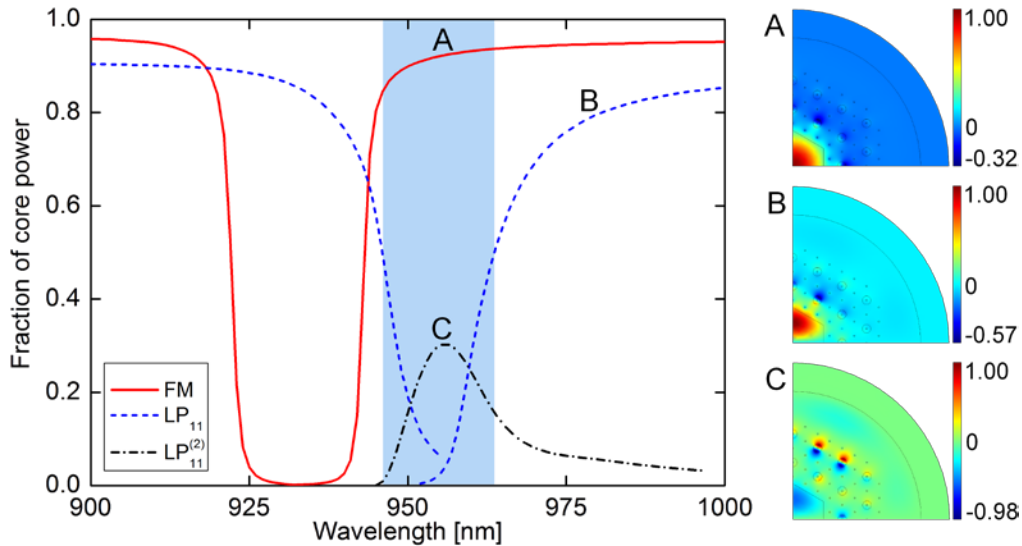


Fig. 2. The fraction of power within the core for the fundamental mode (FM) and first higher order mode (LP_{11}) as a function of wavelength. Within the SM bandwidth (light blue) the power level of an additional LP_{11} -like mode increases ($\text{LP}_{11}^{(2)}$). One normalized transverse component of the electrical field distributions of the modes at A, B and C are seen to the right.

In [12] Alkeskjold *et al.* measured the transmission spectrum of a passive DMF rod fiber with a pitch of $14.7\ \mu\text{m}$, an index contrast between silica and the up-doped Ge-rings of 2.5×10^{-3} , and an air hole diameter of approximately $0.07 - 0.10$ relative to pitch. The DMF rod fiber is identified to be SM from 1050 nm to 1070 nm, yielding a relative SM bandwidth of 1.9%, corresponding well with the simulations above. This indicates that the applied criterion

for quantifying the SM bandwidth is reasonable. The relative air hole diameters of the fabricated DMF rod fiber varies in the fiber cross-section and some are smaller than the simulated air hole diameter. Together with the slightly larger pitch this contributes to the red-shift in the SM bandwidth of approximately 10%. Uncertainties in the refractive index of the core and the up-doped regions are expected for the fabricated DMF rod fiber. These influence the width of the band of cladding modes that creates the SM bandwidth, the mode spacing between the FM and first HOM and the spectral location of the band gap created by the resonators. Therefore differences on the calculated and measured relative SM bandwidth are expected.

5. Design optimization

The design of the DMF rod fiber should be optimized to yield the largest possible SM bandwidth to enable SM amplification of the shortest possible pulses in an amplifier configuration. In the previous design example, the second band of cladding modes is used for coupling with the first HOM. The influence of the band number on the relative SM bandwidth is investigated by considering the first three bands of cladding modes of the DMF rod fiber. The effective refractive index contrast is the difference between the modal effective refractive index of the simulated structure and the refractive index of silica. This is plotted as a function of wavelength for the first three band gaps created by the Ge-rings in the cladding structure in Fig. 3(a). It shows that the contrast of the cladding modes decreases as a function of wavelength. For short wavelengths the cladding modes are confined to the resonators as the wavelength increases the cladding modes become delocalized and couple to create a band of cladding modes. For wavelengths where the effective refractive index of the cladding modes is lower than the refractive index of silica, the cladding modes couple with the core modes, resulting in avoided crossings. This determines the leaking regions of the core modes and thereby also the SM bandwidth. The number of cladding modes within each cladding band increases with increasing cladding band number due to the mode order of the modes confined to each of the DMF elements [14]. The fraction of core power as a function of wavelength is shown in Fig. 3(b). The band of cladding modes significantly broadens for the first band gap creating a large SM bandwidth but also allowing an additional $LP_{11}^{(3)}$ -like mode, $LP_{11}^{(3)}$, to appear within the leaking region of the first HOM. In Fig. 3(b) it is seen that the power level of mode $LP_{11}^{(2)}$ increases with decreasing cladding band number. Two LP_{11} -like modes appear in the first band gap, where one of them has ~50% power within the core. These modes might influence the SM properties of fabricated DMF rod fibers, as it is imaginable that a LP_{11} -like mode with a large fraction of core power over a certain threshold level will disturb the FM resulting in multimode behavior. However, it should be tested experimentally if these LP_{11} -like modes interfere in measurements. The SM bandwidths in Fig. 3 are determined to 7.9%, 1.8%, and 0.3% for the first, second, and third band of cladding modes respectively. The first band of cladding modes yields the largest SM bandwidth, therefore it must be utilized to couple with the first HOM instead of the second band of cladding modes. However, this moves the SM bandwidth to longer wavelengths, away from a desired center wavelength of 1030 nm, where the Yb emission spectrum peaks.

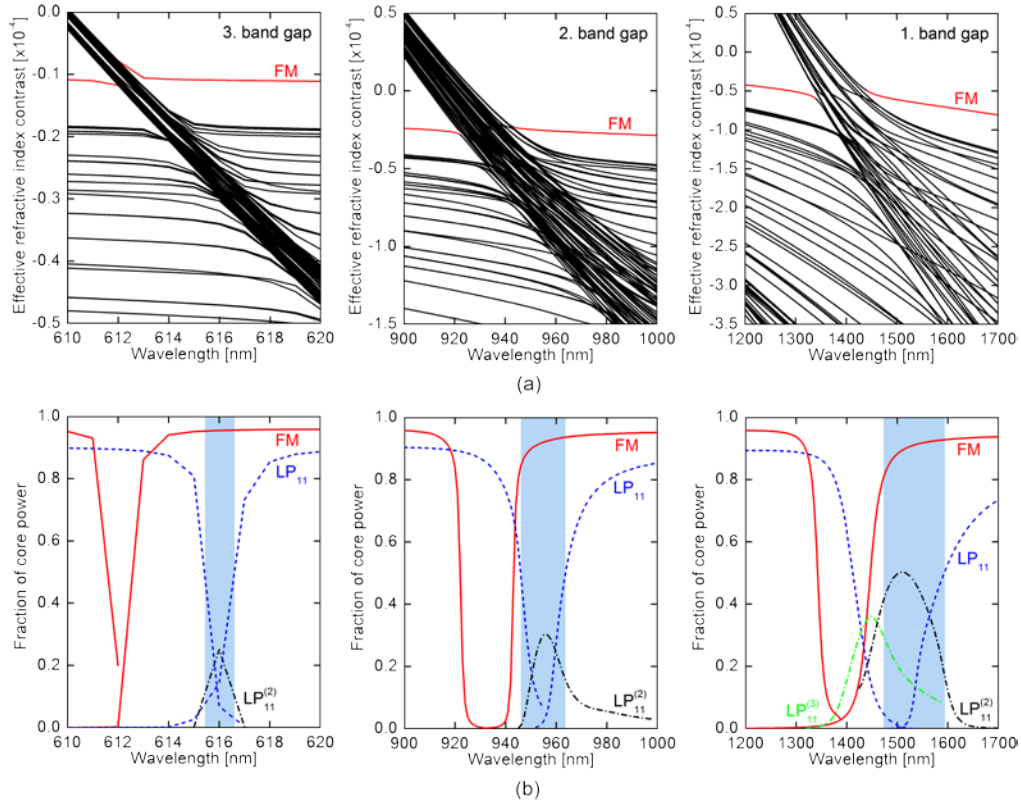


Fig. 3. (a) The effective refractive index contrast as a function of wavelength. The band of cladding modes decreases in effective refraction index as a function of wavelength, and avoided crossings appear between these and the other modes of the DMF rod fiber. (b) The fraction of power within the core for the fundamental mode (solid curve) and LP_{11} -like modes (dashed and dash-dotted curves) as a function of wavelength. Additional LP_{11} -like modes increase in core power within the SM bandwidths. The first band of cladding modes creates the largest SM bandwidth.

The up-doped Ge-rings in the inner cladding structure functions as resonators, which can couple with core modes due to index matching. An effective V-parameter for the resonators is introduced with the characteristic length as the width of the up-doped Ge-rings, w_{dope} , instead of the radius. This is to omit the air hole at the center, since it does not confine the light.

$$V_{\text{res}} = \frac{2\pi w_{\text{dope}}}{\lambda} NA. \quad (2)$$

For the first band of cladding modes the center wavelength is 1532 nm, which yields $V_{\text{res}} = 1.28$. Keeping V_{res} constant and decreasing the center wavelength to 1030 nm yields a refractive index contrast for the resonators of 1.1×10^{-3} , when setting the surrounding refractive index to the index of silica. There are six air holes around each resonator which reduces the effective refractive index of the surrounding silica. In reality the NA in Eq. (2) should be calculated with this effective refractive index, which must be lower at 1520 nm than at 1030 nm, due to the increment in wavelength. Therefore the index contrast of the up-doped Ge-rings is set to 1.2×10^{-3} to compensate the increase in the effective refractive index surrounding the resonators upon scaling from 1532 nm to 1030 nm center wavelength.

The power spectrum showing the fraction of power within the core as a function of wavelength for the first band of cladding modes is seen in Fig. 4. The DMF rod fiber is simulated SM from 990 nm to 1061 nm, which yields a relative SM bandwidth of 6.9%. The center wavelength for the optimized design is at 1026 nm, i.e. close to the maximum gain of

Yb. Again two additional LP_{11} -like modes, $LP_{11}^{(2)}$ and $LP_{11}^{(3)}$, increase in power level within the SM bandwidth, as for the original design with a refractive index contrast of 2.5×10^{-3} utilizing the first band of cladding modes, seen in Fig. 4 as mode C and D. However, their fraction of power within the core is approximately equal to the ones of the original design, and thereby must be dependent on the cladding band number i.e. the band gap number. In Fig. 4 the field distribution within the DMF elements resembles LP_{01} -like modes from a step index fiber if omitting the air hole, verifying that the first band of cladding modes is utilized to create the SM bandwidth.

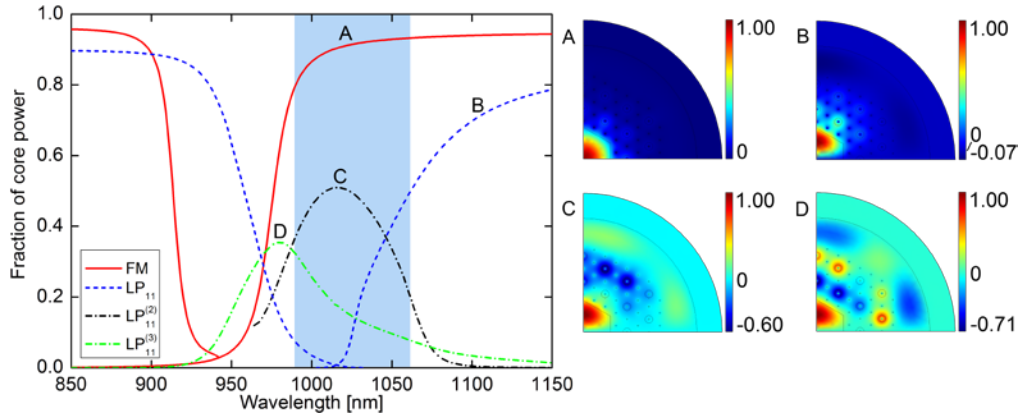


Fig. 4. The fraction of power within the core for the fundamental mode (FM) and first higher order mode (LP_{11}) as a function of wavelength. Within the SM bandwidth (light blue) the power level of two additional LP_{11} -like mode increase ($LP_{11}^{(2)}$ and $LP_{11}^{(3)}$). One normalized transverse component of the electrical field distribution of the modes at A, B, C and D are seen to the right.

The relative SM bandwidth is reduced from 7.9% to 6.9% as the index contrast between the up-doped inclusions and silica is reduced. The confinement of the field within the resonators depends on the index contrast between the up-doped inclusions and silica. Lowering the index contrast causes the field to extend further into the surrounding cladding, and thereby affects the coupling between two adjacent resonators. The smaller relative SM bandwidth for the optimized design compared to the original design is attributed to this change in resonator coupling. Compared to the original DMF rod fiber design the relative SM bandwidth is increased from 1.8% to 6.9% in the simulations, i.e. with almost a factor of four.

6. Fabrication uncertainties

The fabrication uncertainty of the core refractive index of the active DMF rod fiber is approximately $\pm 10^{-4}$ in production. However, the SM bandwidth must have approximately the same center wavelength in a fabricated DMF rod fiber despite uncertainties of the core refractive index. Therefore the air hole diameter is varied during the fiber draw to compensate for core refractive index changes. A lower core refractive index than expected corresponds to a redshift of the SM bandwidth, whereas a higher core refractive index corresponds to a blueshift. The former is compensated by increasing the air hole diameter, i.e. blueshifting the SM bandwidth, and the latter is compensated by decreasing the air hole diameter. A minimum air hole diameter of $\sim 1.5 \mu\text{m}$ corresponding to $\sim 0.1\lambda$ is required due to reproducibility of the fibers. Thus the optimized fiber design in Sec. 5 represents the ideal case.

This section presents parameters to be targeted during the fiber draw taking limiting fabrication uncertainties into consideration. Both a positive and negative core refractive index contrast must be compensated; therefore the relative air hole diameter is increased to 0.15 for the case of a core refractive index equal to the refractive index of silica. This shifts the SM bandwidth to shorter wavelengths, which is compensated by increasing the relative resonator diameter from 0.60 to 0.69. Three index contrasts between the core refractive index and the

refractive index of silica are considered: $\Delta n = 10^{-4}$, $\Delta n = 0$ and $\Delta n = -10^{-4}$. The relative air hole diameter is altered accordingly in three steps: $d/\Lambda = 0.1$, $d/\Lambda = 0.15$ and $d/\Lambda = 0.2$, while all other parameters are kept constant. The power spectra are seen in Figs. 5(a), 5(b), and 5(c) with SM bandwidths of 5.1%, 5.4% and 5.8% respectively, seen as the light blue area, having center wavelengths of 1024 nm, 1016 nm and 1028 nm respectively. This is summarized in Table 1. The design of the DMF rod fiber has the ability to compensate fabrication uncertainties in the core refractive index while maintaining the SM properties. The relative resonator diameter of the optimized design in Sec. 5 must be increased to 0.69 and relative air hole diameters in the range 0.1 to 0.2 should be targeted during the fiber draw to guarantee an active DMF rod fiber with a SM bandwidth having a center wavelength close to the maximum Yb gain.

Also, noticed in Fig. 5, the power levels of the additional LP_{11} -like modes decrease as the core refractive index decreases. Therefore it could be an advantage to decrease the core refractive index in the fabricated DMF rod fiber to increase the SM bandwidth and to lower the power level of other LP_{11} -like modes that might disturb the SM properties. The notch of the FM around 883 nm in Fig. 5(c) corresponds to an avoided crossing.

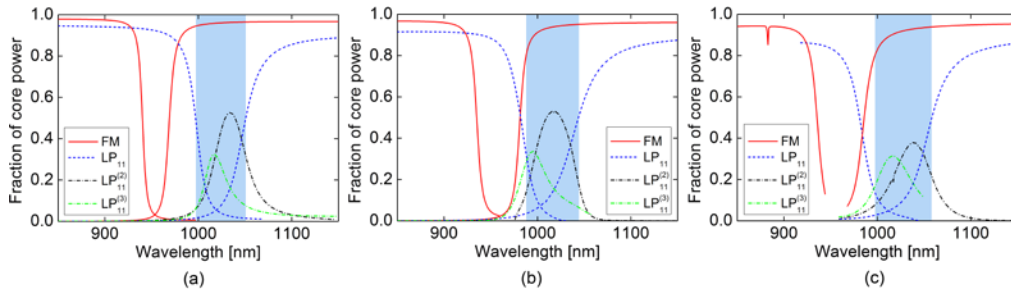


Fig. 5. Power spectra for estimating fabrication parameters to be targeted during the fiber pull. Three values of the refractive index contrast, Δn , is considered, where the relative air hole diameter is altered accordingly: (a) $\Delta n = 10^{-4}$ and $d/\Lambda = 0.1$, (b) $\Delta n = 0$ and $d/\Lambda = 0.15$, and (c) $\Delta n = -10^{-4}$ and $d/\Lambda = 0.2$.

Table 1. Design Parameters and Obtained Single Mode Bandwidths for Three Values of the Core Refractive Index and the Air Hole Diameter

Δn	d / Λ	SM bandwidth [%]	SM center wavelength [nm]
10^{-4}	0.1	5.1	1024
0	0.15	5.4	1016
-10^{-4}	0.2	5.8	1028

7. Pitch scaling

Changing the pitch of the DMF rod fiber corresponds to scaling Maxwell's equations, causing the SM bandwidth to scale accordingly. This allows the spectral location of the SM bandwidth to be moved to shorter or longer wavelengths, which is utilized during the fiber draw. However, nothing is gained or lost in the relative size of the SM bandwidth, since the band gap width and spectral location change accordingly. In this section the effect of the pitch on the relative size of the SM bandwidth is investigated, when keeping the physical size of air holes and up-doped Ge-rings constant. The air hole diameter is 1.45 μm and the Ge-ring radius is determined from Eq. (1). Thereby investigating if the core area can be increased by increasing the pitch and also maintain the SM properties of the DMF rod fiber. Increasing the pitch increases the distance between the air holes and up-doped Ge-rings. The optimized design in Sec. 5 with a pitch of 14.5 μm is considered, changing only the pitch in three steps: 11.5 μm , 17.5 μm , and 20.5 μm , corresponding to core diameters of 67 μm , 103 μm and 120 μm , respectively.

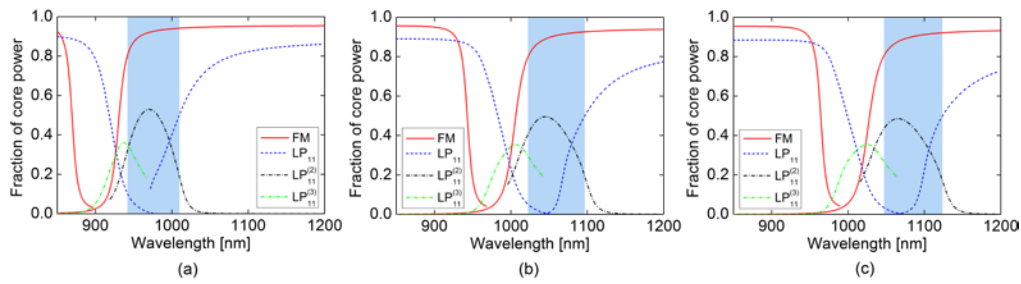


Fig. 6. The fraction of power within the core as a function of wavelength for the optimized design with three different values of the pitch: (a) 11.5 μm , (b) 17.5 μm , and (c) 20.5 μm , having relative single mode bandwidths of 6.9%, 6.9%, and 7.0% respectively.

Figure 6 shows the fraction of power in the core as a function of wavelength for the three values of pitch. The relative SM bandwidth is approximately constant at 6.9%, 6.9%, and 7.0% for a pitch of 11.5 μm , 17.5 μm , and 20.5 μm respectively. Even though the pitch is significantly changed yielding a maximum core diameter of 120 μm , the SM bandwidth stays approximately constant. The physical size of the resonators and air holes are constant, this means that the spectral location of the band gap should remain unchanged. As the pitch increases the effective NA between core and cladding is reduced and the design becomes very sensitive to refractive index uncertainties. There is a slight shift of the center wavelength of the SM bandwidth to longer wavelengths as the pitch increases in Fig. 6. Increasing the pitch moves the air holes away from the resonators, which results in a lower field overlap with the air holes of the cladding modes confined to the resonators. This increases the effective refractive index of the cladding modes moving the avoided crossings of the cladding modes with core modes to longer wavelengths. Also, the fraction of core power decreases slightly as the pitch increases, since the core modes become less confined to the core. The absolute distance between the core and the first surrounding air holes increases as the pitch increases, allowing the core modes to penetrate deeper into the cladding yielding a lower core overlap.

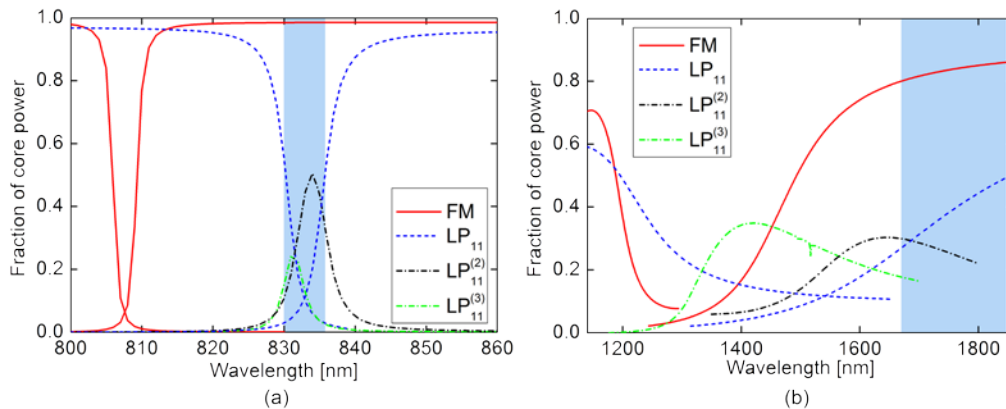


Fig. 7. The fraction of modal power within the core as a function of wavelength. The pitch is 20.5 μm and the core refractive index is up-doped with 10^{-4} in (a) and down-doped with -10^{-4} in (b), which significantly changes the single mode bandwidth (light blue area).

Increasing the pitch makes the DMF rod fiber extremely sensitive to core refractive index changes. Two changes in the refractive index of the core are considered for the DMF rod fiber with the optimized design and a pitch of 20.5 μm , this is to see the effects of the fabrication uncertainties in the core refractive index. In Fig. 7(a) the core is up-doped with 10^{-4} and in Fig. 7(b) the core is down-doped with -10^{-4} relative to the refractive index of silica. The DMF rod fiber is SM from 830 nm to 835 nm in (a) and from 1670 nm to 1854 nm in (b) yielding relative SM bandwidths of 0.6% and 10.4% respectively. Up-doping the core

blueshifts and significant decreases the SM bandwidth to approximately 10% of the index matched core. Opposite for the down-doped core, where the SM bandwidth is increased to 150% of the index matched core. Down-doping the core makes the core modes less confined as seen in Fig. 7(b) as the lower core overlap, which decreases the modal gain in the active DMF rod fiber. These core refractive index changes illustrates how sensitive the DMF rod fiber becomes to core index changes as the pitch and thereby core diameter is increased, summarized in Table 2. DMF rod fibers having a large a pitch, such as $> 20 \mu\text{m}$, requires better control of core refractive index, since a core refractive index uncertainty of $\pm 10^{-4}$ cannot be compensated by the DMF structure, while maintaining a relatively large SM bandwidth. The required precision is currently under evaluation.

Table 2. The Single Mode Bandwidth for Four Values of the Pitch When the Air Hole Diameter Is Fixed at $1.45 \mu\text{m}$ *

$\Lambda [\mu\text{m}]$	Δn	SM bandwidth [%]
11.5	0	6.9
14.5	0	6.9
17.5	0	6.9
20.5	0	7.0
20.5	10^{-4}	0.6
20.5	-10^{-4}	10.4

*The core refractive index is changed with $\Delta n = \pm 10^{-4}$ for at pitch of $20.5 \mu\text{m}$.

8. Conclusion

The cross-section of the DMF rod fiber was set up numerically to determine modal properties by the finite element method. Especially the SM bandwidth was determined considering core overlap of the FM and first HOM, as the spectral region where the first HOM couples with cladding modes, while the FM is still confined to the core. The simulated relative SM bandwidth agreed well with the measured SM bandwidth of the original DMF rod fiber design. The band of cladding modes was identified as the second band resembling LP_{11} -like modes in each resonator for short wavelengths. The DMF rod fiber design was numerically optimized by utilizing the first band of cladding modes instead of the second band to couple with core modes. This resulted in a fourfold increase of the SM bandwidth from 1.8% to 6.9%, covering a large fraction of the Yb emission band that could include wavelengths of 1030 nm and 1064 nm. Also fabrication uncertainties in the core refractive index of $\pm 10^{-4}$ were considered and could be compensated by altering the air hole diameter from 0.1Λ to 0.2Λ , while maintaining relative SM bandwidths from 5.1% to 5.8%. One possibility to increase the core diameter is to increase the pitch, while fixing the physical size of air holes and up-doped Ge-rings in the cladding structure. This was investigated and it was seen that the SM bandwidth was approximately constant as the pitch increased. However, the larger pitch resulted in a fiber design not suitable for production, since core refractive index changes could not be compensated without significantly reducing the SM properties and FM core overlap.